International Journal of Nanomedicine

Dovepress
open access to scientific and medical research

Open Access Full Text Article

ORIGINAL RESEARCH

Mitochondria-Modulating Porous Se@SiO_2 Nanoparticles Provide Resistance to Oxidative Injury in Airway Epithelial Cells: Implications for Acute Lung Injury

This article was published in the following Dove Press journal:
International Journal of Nanomedicine

Muyun Wang[1,*]
Kun Wang[1,*]
Guoying Deng[2,*]
Xijian Liu[3]
Xiaodong Wu[1]
Haiyang Hu[4]
Yanbei Zhang[5]
Wei Gao[1]
Qiang Li[1]

[1]Department of Pulmonary and Critical Care Medicine, Shanghai East Hospital, Tongji University, Shanghai 200120, People's Republic of China; [2]Department of Orthopedics, Shanghai General Hospital, Shanghai Jiao Tong University School of Medicine, Shanghai 201620, People's Republic of China; [3]College of Chemistry and Chemical Engineering, Shanghai University of Engineering Science, Shanghai 201620, People's Republic of China; [4]Department of Cardiothoracic Surgery, Shanghai General Hospital, Shanghai Jiao Tong University School of Medicine, Shanghai 201620, People's Republic of China; [5]Department of Geriatric Pulmonary and Critical Care Medicine, The First Affiliated Hospital of Anhui Medical University, Anhui 230022, People's Republic of China

*These authors contributed equally to this work

Background: Mitochondrial dysfunction played a vital role in the pathogenesis of various diseases, including acute lung injury (ALI). However, few strategies targeting mitochondria were developed in treating ALI. Recently, we fabricated a porous Se@SiO_2 nanoparticles (NPs) with antioxidant properties.

Methods: The protective effect of Se@SiO_2 NPs was assessed using confocal imaging, immunoblotting, RNA-seq, mitochondrial respiratory chain (MRC) activity assay, and transmission electron microscopy (TEM) in airway epithelial cell line (Beas-2B). The in vivo efficacy of Se@SiO_2 NPs was evaluated in a lipopolysaccharide (LPS)-induced ALI mouse model.

Results: This study demonstrated that Se@SiO_2 NPs significantly increased the resistance of airway epithelial cells under oxidative injury and shifted lipopolysaccharide-induced gene expression profile closer to the untreated controls. The cytoprotection of Se@SiO_2 was found to be achieved by maintaining mitochondrial function, activity, and dynamics. In an animal model of ALI, pretreated with the NPs improved mitochondrial dysfunction, thus reducing inflammatory responses and diffuse damage in lung tissues. Additionally, RNA-seq analysis provided evidence for the broad modulatory activity of our Se@SiO_2 NPs in various metabolic disorders and inflammatory diseases.

Conclusion: This study brought new insights into mitochondria-targeting bioactive NPs, with application potential in curing ALI or other human mitochondria-related disorders.

Keywords: mitochondrial dysfunction, porous Se@SiO_2 nanoparticles, acute lung injury, anti-oxidative injury, anti-inflammation

Introduction

Mitochondria are elongated double-membrane-bound organelles with independent self-replicating genome and can be universally found in the cytoplasms of almost all eukaryotic cells. As the most capital organelle, mitochondria are able to "energize" cells with adenosine triphosphate (ATP), as well as involve in various physiological processes including redox signaling, programmed cell death (apoptosis) and calcium flux.[1,2] It has been well appreciated that mitochondrial dysfunction played an essential role in the pathogenesis of multiple metabolic and age-related disorders, such as diabetes, obesity, hypertension, and neurodegenerative diseases.[3] Recently, studies claimed that mitochondrial dysfunction also contributed to the

Correspondence: Wei Gao; Qiang Li
Email grace19881118@126.com; liqressh2@hotmail.com

submit your manuscript | www.dovepress.com
DovePress
http://doi.org/10.2147/IJN.S240301

development of several inflammatory lung diseases, including acute lung injury (ALI), or its more severe stage, acute respiratory distress syndrome (ARDS).[4,5]

ALI/ARDS is a common respiratory critical syndrome with clinical manifestations of acute, progressive respiratory distress, and multiorgan dysfunction.[6] Despite significant progress in intensive care medicine and organ supportive therapy, the mortality of ALI/ARDS remained over 40% throughout the world.[7] During the pathogenesis of this disorder, overwhelming uncontrolled innate immune system released large amounts of inflammatory cytokines, which induced mitochondrial dysfunction, manifesting as membrane destabilization or rupture, calcium disorder, oxidative phosphorylation inhibition, and reactive oxygen species (ROS) overload. These changes eventually led to microvascular endothelial–alveolar epithelial barrier disruption, neutrophil infiltration, pulmonary edema formation and gas exchange impairment.[6,8] Airway epithelium is continuously considered the first line of host defense against noxious insults. Bundles of studies observed mitochondrial dysfunction of airway epithelial cells (AECs) in ALI/ARDS.[5,9,10] Moreover, rescuing AECs from mitochondrial dysfunction through mitochondria transferring relieved LPS-induced ALI.[11] A more recent report also affirmed that compensation for mitochondrial impairment by enhancing cellular glycolytic activity could protect airway epithelium from acute injury.[10] Therefore, preventing AECs from mitochondrial impairment might provide a promising therapeutic target for ALI/ARDS.

In this regard, numerous "drugs" have been documented over the years ranging from mitochondria-targeted cation to triphenylphosphonium (TPP)-conjugated antioxidants.[3,12-14] Among them, mitochondria-targeting nanoparticles (NPs) emerged as potential therapeutic alternations due to their improved cell targeting capabilities, desired biodistribution, and better biocompatibilities.[15–17] Despite the growing evidence of therapeutic outcomes by inducing mitochondrial-mediated tumor cell apoptosis,[2,18] the application of nanodevices on the maintenance of mitochondrial homeostasis was quite limited. TPP-conjugated ceria (TPP-ceria) NPs have been developed to mitigate amyloid beta-induced mitochondrial morphology damage and excessive oxidative stress, thus providing potential therapeutic candidate for Alzheimer's disease.[19] However, few studies were about the development of "nano-drug" which could modulate mitochondrial homeostasis and further alleviate ALI/ARDS so far.

Selenium (Se), an essential trace nutrient in humans with multiple biological functions, has been considered a stable and economic antioxidant.[20] However, Se may also exert cytotoxicity through generating superoxide along with catalyzing thiols oxidation.[21] Rapid advances in nanotechnology have provided unconventional solutions to overcome the obstacles that hinder the clinical use of Se-containing medicine. We have recently developed a novel class of porous Se@SiO_2 nanoparticles (NPs) with extremely low cytotoxicity and preferred biocompatibility. The novel nanodevice released Se slowly and sustainably and was reported to attenuate oxidative stress in several disease models.[22–24] As is well known, mitochondrial dysfunction is the major source of ROS overload.[4] Therefore, we hypothesized that the porous Se@SiO_2 NPs might alleviate oxidant injury in ALI/ARDS via modulating mitochondrial dysfunction.

In the present study, we found that the porous Se@SiO_2 NPs largely enhanced the resistance of AECs to lipopolysaccharide (LPS)-induced oxidative injury through maintaining mitochondrial ROS-scavenging activity and ameliorating mitochondrial dynamics. The NPs also presented potential therapeutic application against LPS-induced ALI in a classical mouse model. Furthermore, Gene Ontology (GO) enrichment and Kyoto Encyclopedia of Genes and Genomes (KEGG) pathway analysis provided additional evidence for the broad modulatory activity of the Se@SiO_2 NPs and their potential for clinical translation in various metabolic disorders and inflammatory diseases.

Materials and Methods

Additional details are provided in the Supplementary Material - Methods.

Synthesis and Characterization of the Porous Se@SiO_2 NPs

The porous Se@SiO_2 NPs were synthesized according to the methods used in our previous research.[23] The porous Se@SiO_2 NPs were prepared as schematically illustrated in Scheme 1. Characterization of the NPs was achieved by using a transmission electron microscopy and a D/max-2550 PC X-ray diffractometer.

Cell Culture and Processing

Airway epithelial cell line (Beas-2B) was purchased from Shanghai Institutes for Biological Sciences, China Academy

of Science (Shanghai, China). Details are shown in the Supplementary Material - Cell culture and processing.

In vitro Cytotoxicity of the Se@SiO_2 NPs

Details are shown in the Supplementary Material - In vitro cytotoxicity of the Se@SiO_2 NPs.

Detection of Intracellular ROS and Mitochondrial ROS

Intracellular and mitochondrial ROS were detected using CellROX™ deep red reagent and MitoSOX™ Red probe, respectively. More details are shown in the Supplementary Material - Detection of intracellular ROS and mitochondrial ROS.

Evaluation of Mitochondrial Respiratory Chain (MRC) Activities

The activities of mitochondrial respiratory chains were measured by MRC Complex I–V Activity Assay Kit according to their manufacturer's instructions. More details are shown in the Supplementary Material - Evaluation of mitochondrial respiratory chain (MRC) activities.

Western Blotting (WB) Analysis

Details are shown in the Supplementary Material - Western blotting (WB) analysis.

Measurement of Mitochondrial Morphology and Activity

Details are shown in the Supplementary Material - Measurement of mitochondrial morphology and activity.

RNA-Sequencing and Data Analysis

Total RNAs were extracted using TRIzol-based method and the following procedures were conducted by Genergy Biotechnology Co. Ltd. (Shanghai, China). Details are shown in the Supplementary Material - RNA-Sequencing and data analysis.

Establishment of Acute Lung Injury Murine Model

ALI mice model experiments were conducted following the protocols of Shanghai Committee for the Accreditation of Laboratory Animal. All processes have been approved by Shanghai General Hospital Institutional Review Board (the Permit Number, 2018KY201. Shanghai, China). All the operations were performed after sodium pentobarbital anesthesia with all efforts made to minimize mice suffering. Details are shown in the Supplementary Material - Establishment of acute lung injury murine model.

Bronchoalveolar Lavage Fluid (BALF) Acquisition and Analysis

Details are shown in the Supplementary Material - Bronchoalveolar lavage fluid (BALF) acquisition and analysis.

Histological Analysis of Lung Injury

All sections were assessed by two independent physicians who were blinded to the treatment group according to international standards.[25] Additional details are shown in the Supplementary Material - Histological analysis of lung injury.

Lung Wet-to-Dry (W/D) Weight Ratio

Details are shown in the Supplementary Material - Lung wet-to-dry (W/D) weight ratio.

Statistical Analysis

The results were analyzed by the use of GraphPad Prism 7 software. Data were managed through One-Way ANOVA and Bonferroni's post hoc test (for equal variance) or Dunnett's T3 post hoc test (for unequal variance). Quantitative data were described as mean ± standard error (± SEM). The difference was defined statistically significant only when $p < 0.05$.

Results

Characterization of the Porous Se@SiO_2 Nanoparticles

The porous Se@SiO_2 NPs were prepared as schematically illustrated in Figure 1A. The phase structure of the NPs was assessed by the X-ray diffractometer (XRD) pattern (Figure 1B). Various definite characteristic peaks in Se@SiO_2 NPs, including (100), (011), (012) and (021), suggested their hexagonal phase, using the standard Se phase (JCPDS card No.65–1,876) as a reference. Attributed to their irregular silica coating, the XRD pattern demonstrated a significant increase in the low angle region of our Se@SiO_2 NPs (Figure 1B). Additionally, we adopted a transmission electron microscopy (TEM) method to observe the morphology and size of Se@SiO_2 NPs. As shown in Figure 1C and D, the average diameter of NPs was about 55 nm, in which lots of

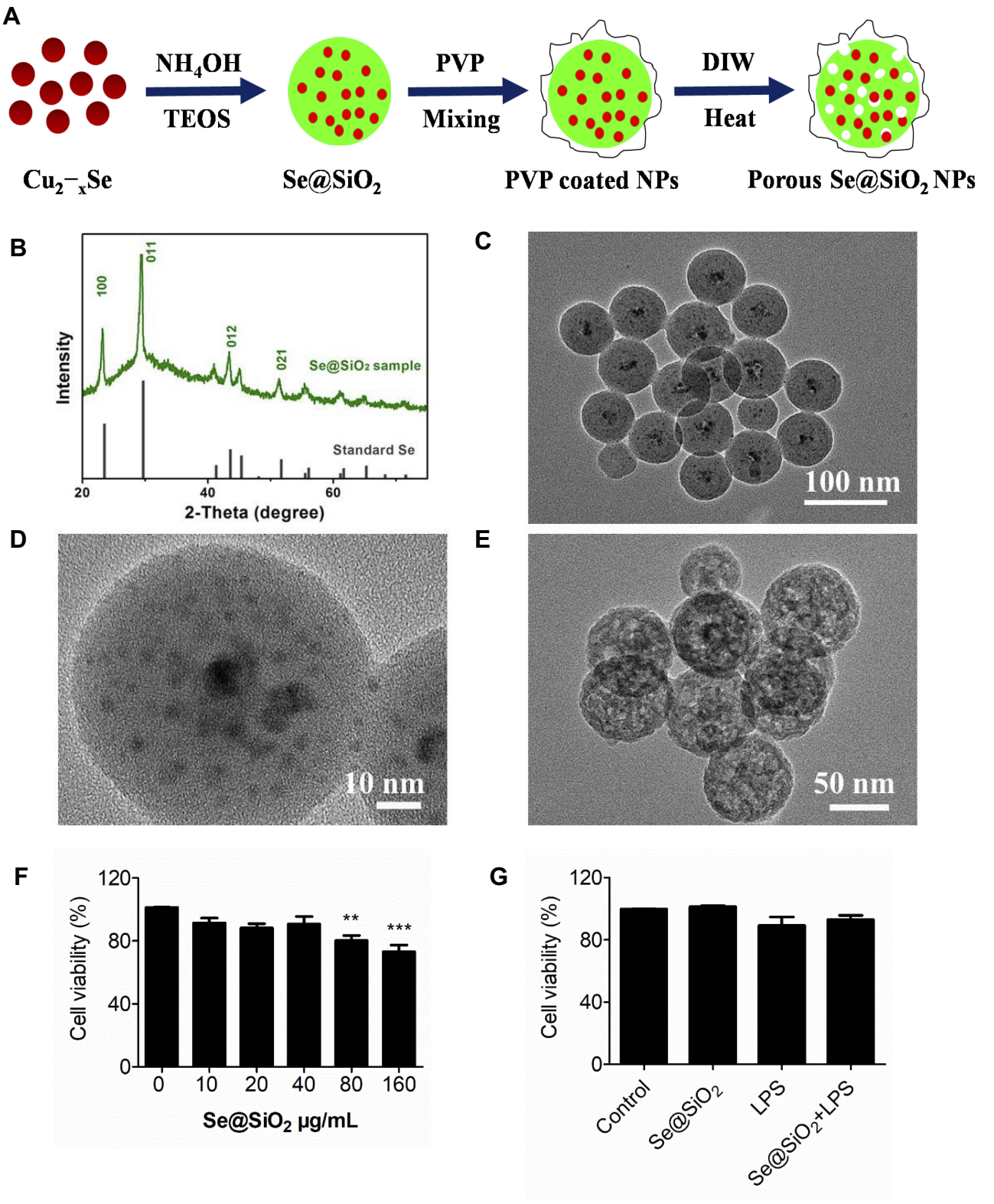

Figure 1 Characterization of the porous $Se@SiO_2$ nanoparticles. (**A**) Fabrication of porous $Se@SiO_2$ nanoparticles (NPs). (**B**) The XRD pattern of porous $Se@SiO_2$ NPs as well as the typical hexagonal phase of selenium (JCPDS card No. 65–1,876). (**C** and **D**) Low- (**C**) and high-magnified (**D**) TEM images of the NPs before heat water treatment. (**E**) TEM images of porous $Se@SiO_2$ NPs after the treatment with heat water at 95°C. (**F**) The effect of various concentrations of NPs on the cell viability in cultured airway epithelial cells (the Beas-2B cell line). (**G**) The effect of LPS stimulation (10 ng/mL) and NP treatments (10 μg/mL) on the cell viability in Beas-2B cells. $^{**}p < 0.01$, $^{***}p < 0.001$.

Abbreviations: DIW, deionized water; TEOS, tetraethyl orthosilicate.

irregular quantum dots (less than 5 nm) distributed from center to the surface. After treating with the hot water, Se@SiO_2 NPs presented the porous structure (Figure 1E). Coated with PVP, the Se quantum dots on the surface of or inside silica shell twined around them and could be released slowly along with the entrance of PVP into aqueous solution. Besides, we also examined the size distribution and zeta potential by the use of dynamic light scattering (DLS). The hydrodynamic diameter of Se@SiO_2 NPs was ~127 nm, which a little larger than that of TEM. Meanwhile, their zeta potential was ~-19.0 mV due to the OH groups on the surface of the silica. The physiological stability and Se quantum dots release of the Se@SiO_2 NPs have been studied in our previous research.[23]

Subsequently, we determined the cellular toxicity of Se@SiO_2 NPs on Beas-2B cells using the CCK-8 assay (Figure 1F and G). Cells were co-cultured with various concentrations of Se@SiO_2 NPs, ranging from 0 μg/mL to 160 μg/mL. Compared to the control group, cellular viability of Beas-2B cells was not affected by the Se@SiO_2 NPs under 40 μg/mL (Figure 1F). Choosing the concentration of 10 μg/mL, we further demonstrated that the NPs did not show significant inhibitory effect on cell viability combined with LPS (10 ng/mL) (Figure 1G).

The Porous Se@SiO_2 NPs Enhanced the Resistance of Airway Epithelial Cells to LPS-Induced Oxidative Injury

In previous studies, porous Se@SiO_2 NPs have been reported to combat oxidative stress in several disease models due to the slow-released Se.[22,24,26] Herein, we assessed the effect of 10 μg/mL Se@SiO_2 on LPS-induced oxidative damage in Beas-2B cells firstly. Cells pretreated with NPs produced less ROS in response to 10 ng/mL LPS than those without Se@SiO_2 pretreatment (Figure 2A). This was associated with decreased phosphorylation of the NF-κB subunit p65, p38 signaling and extracellular-signal regulated kinase (ERK1/2) signaling in the mitogen-activated protein kinase (MAPK) pathways (Figure 2B and see Supplementary Material-Figure S1A-C). Furthermore, Se@SiO_2 significantly reversed the inhibition of LPS on expression of nuclear factor erythroid 2-related factor 2 (NRF2) and the downstream target NAD(P)H quinone dehydrogenase-1 (NQO1), indicating an enhanced endogenous antioxidant response in Beas-2B cells (Figure 2C and see Supplementary Material-Figure S1D-E). Meanwhile, the expression of tight junction marker zonula occludens-1 (ZO-1) and the adherence junction marker E-cadherin (E-Ca) was also upregulated by Se@SiO_2 NPs compared with LPS group (Figure 2C, see Supplementary Material-Figure S1F-G). These suggested that the increased antioxidant activity and cellular tight junction followed Se@SiO_2 treatment could prevent AECs from LPS-induced damage.

To comprehensively evaluate the protective activity of porous Se@SiO_2 NPs, we used RNA-Seq method to study the global effects of the NPs on LPS-mediated transcriptome transformation of human AECs (Beas-2B cells). A gene expression heat map (Figure 2D) and principal component analysis (PCA) of all differentially expressed genes (Figure 2E) demonstrated a distinct separation between the control and LPS-stimulated group. Moreover, NPs treatment globally shifted LPS-induced gene expressions profile closer to the untreated controls, with more up-regulated genes than down-regulated genes (see Supplementary Material-Figure S2). As shown in Figure 2D, top 50 differentially expressed genes with Se@SiO_2 pretreatment displaying a similar pattern to the control group. Among them, many were associated with the morphological integrity and functional stability of mitochondria.[27–35]

Porous Se@SiO_2 NPs Maintained Mitochondrial ROS-Scavenging Activity in an ALI Cell Model Induced by LPS

As mentioned above, mitochondria served as the capital organelle in the regulations of both energy and free radical metabolism. Mitochondria dysfunction has long been considered playing a crucial part in oxidative injury and contributing to various pathological processes, including ALI/ARDS. Herein, we speculated that the increased resistance of epithelial cells to LPS-induced oxidative injury might be associated with the stable mitochondrial ROS-scavenging activity modulated by porous Se@SiO_2 NPs. In this study, we adopted a living cell-permeable indicator, MitoSOX to analyze mitochondria-specific ROS by a confocal microscope or microplate reader. As shown in Figure 3A, 24 h exposure of LPS elevated mitochondrial ROS levels in Beas-2B cells, while pretreatment with Se@SiO_2 NPs significantly reduced the mitochondrial ROS. NPs addition alone had no effect on mitochondrial ROS compared to the control group. Such results were also confirmed by a microplate reader quantificationally (Figure 3B).

To further examine the effects of Se@SiO_2 NPs on mitochondrial ability responsible for cellular homeostasis, we detected the activities of several redox enzymes within mitochondria, MRC complex I–V in AECs. LPS exposure for 24

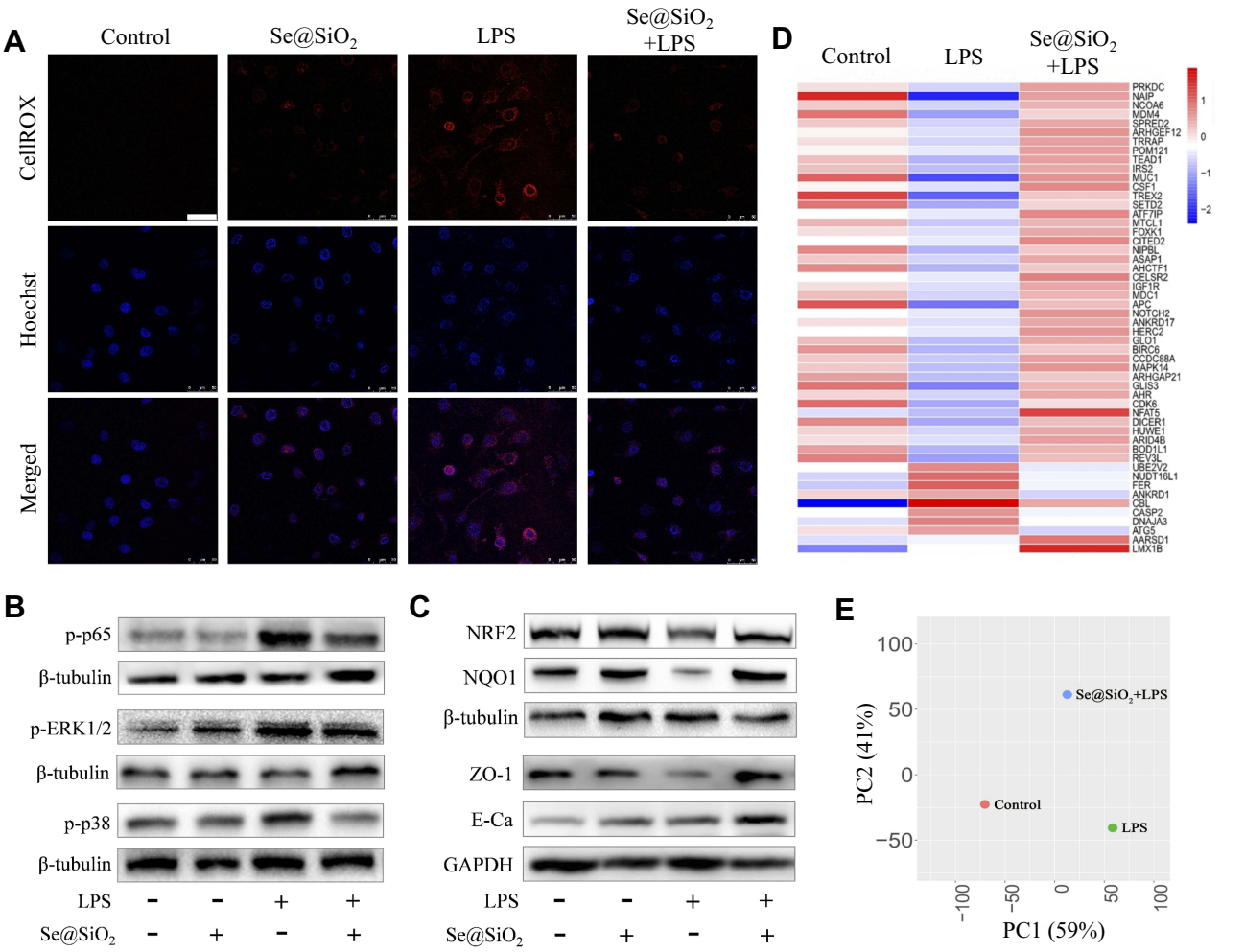

Figure 2 Porous Se@SiO_2 NPs enhanced the resistance of AECs to LPS-induced oxidative injury. (**A**) Representative confocal images showing the effect of Se@SiO_2 NPs on LPS-induced oxidative stress in Beas-2B cells; the intracellular ROS was stained with CellROX™ deep red reagent, shown in red, and the nucleus was stained with Hoechst, displayed in blue. All the images were caught at the same magnifications. The scale bar represents 50 μm. (**B** and **C**) WB showing the effect of Se@SiO_2 NPs on the increased expression of p-p65, p-ERK1/2 (MAPK), and p-p38 (MAPK) (**B**), as well as the reduced expression of NRF2, NQO1, ZO-1, and E-Ca (**C**) after 24 h of LPS stimulation. (**D** and **E**) Impact of porous Se@SiO_2 NPs on the RNA-Seq transcriptome analysis of LPS-challenged human AECs; (**D**) The differential expression profiles of the top 50 genes. (**E**) the PCA plot. NP concentration = 10 μg/mL, LPS = 10 ng/mL.

h decreased the activity of MRC complex I (Figure 3C). While Se@SiO_2 NPs addition significantly elevated the activities of MRC complex I, III, and V after LPS stimulation (Figure 3C–E). These data indicated an important role of Se@SiO_2 NPs in maintaining mitochondrial ROS-scavenging function in ALI cell model induced by LPS.

Porous Se@SiO_2 NPs Ameliorated Mitochondrial Dynamics Under LPS Stimulation in Airway Epithelial Cells

As the ROS-scavenging function of mitochondria optimized by Se@SiO_2 NPs in LPS-stimulated AECs, we next estimated mitochondrial morphology and activity in each group. As shown in Figure 4A, mitochondrial morphology was observed by labeling with MitoTracker probe under a confocal laser microscope. The Beas-2B cells in either control group or NPs-treated group had numerous mitochondria, spread in the perinuclear regions with long lengths. By contrast, mitochondria in LPS-stimulated cells broke seriously, debris increased, and grids decreased. Mitochondrial structure within cells pre-treated with Se@SiO_2 NPs was near to the normal when compared with the model group (Figure 4A). In order to detect mitochondrial activity, we analyzed the fluorescence intensity of MitoTracker in each group. Data showed that relative fluorescence intensity of the mitochondria in LPS-treated group decreased significantly in contrast to the control group. Moreover, the fluorescence of cells in NPs

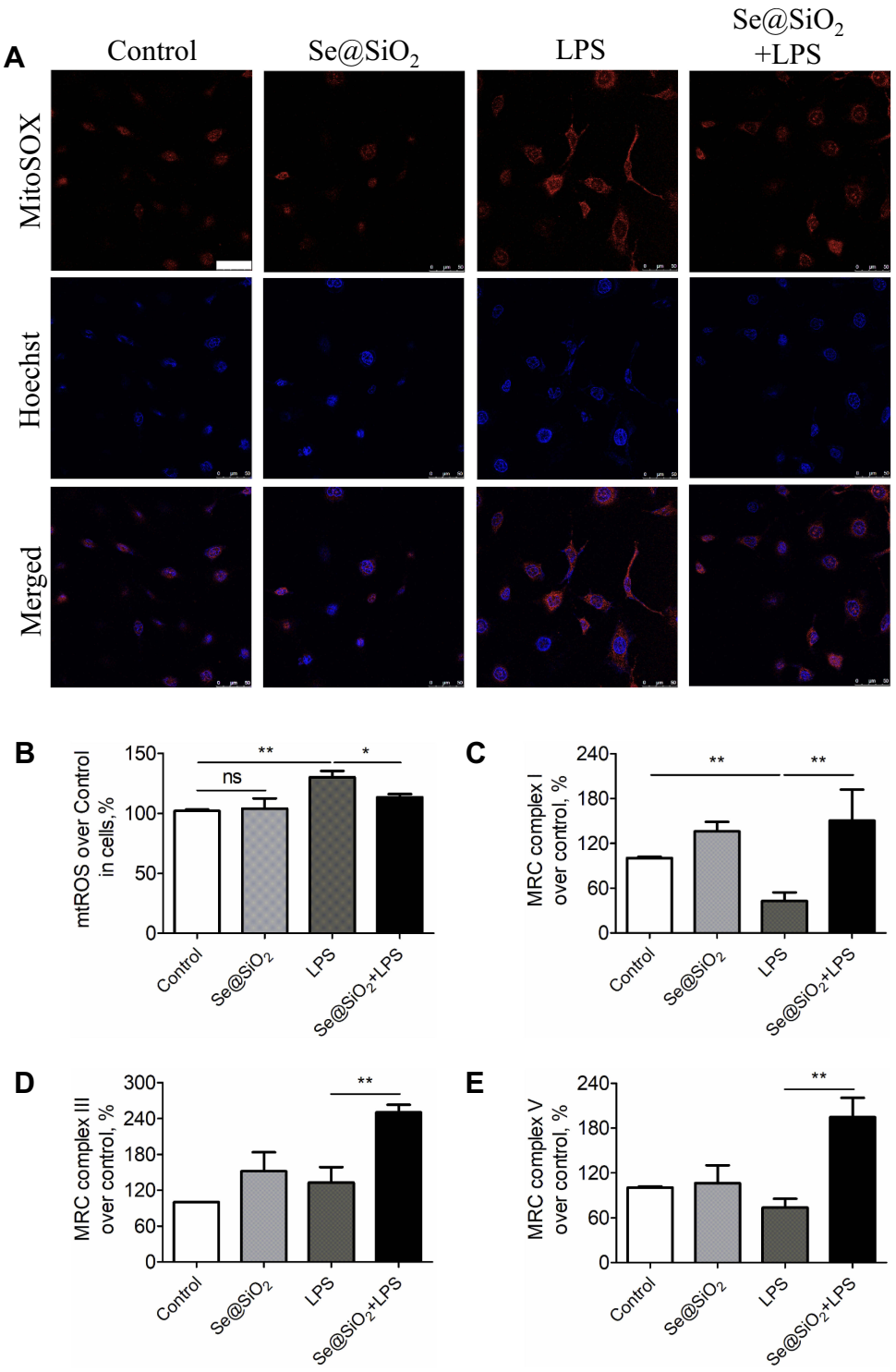

Figure 3 Porous Se@SiO_2 NPs maintained mitochondrial ROS-scavenging activity in LPS-induced human AECs. (**A**) Representative confocal images showing the effect of Se@SiO_2 NPs on LPS-induced mitochondria-specific ROS in Beas-2B cells; the mitochondrial ROS was stained with MitoSOX™ Red probe, displayed in red, and the nucleus was stained with Hoechst dye, displayed in blue. All the images were caught at the same magnifications. The scale bar represents 50 μm. (**B**) Quantification of mitochondrial ROS level by a microplate reader. (**C**–**E**) The effect of LPS and Se@SiO_2 NPs on the activity of mitochondrial respiratory chain (MRC) complexes I (**C**), III (**D**) and V (**E**) in Beas-2B cells. NP concentration = 10 μg/mL, LPS = 10 ng/mL. *$p < 0.05$, **$p < 0.01$.

pretreated group displayed much stronger intensity than the model group, suggesting mitochondrial activity elevated following Se@SiO_2 addition (Figure 4B).

Mitochondrial morphology was also analyzed by TEM. Pretreatment with Se@SiO_2 NPs restored the severe break, cristae disruptions, and vacuolar shape in LPS-challenged

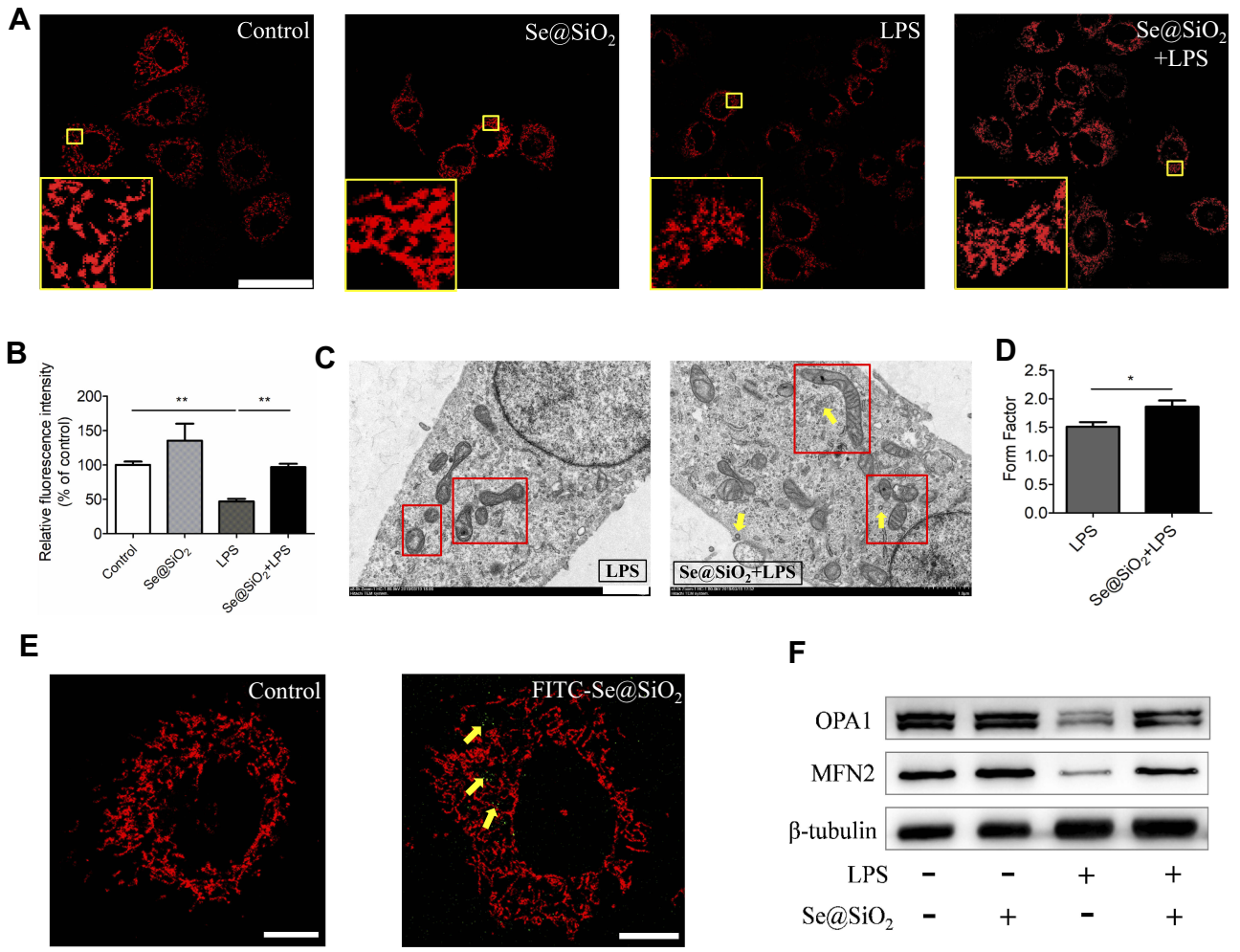

Figure 4 Porous Se@SiO_2 NPs ameliorated mitochondrial dynamics under LPS stimulation in Beas-2B cells. (**A**) Representative confocal images showing changes in the mitochondrial morphology of Beas-2B cells; The mitochondria were labeled with MitoTracker Red CMXRos (MTR) staining solution and displayed in red. All the images were caught at the same magnifications. The scale bar represents 50 μm. Yellow boxes indicated local amplification of the mitochondria. (**B**) Quantification of the red fluorescence intensity in each cell exhibiting the changes in the activity of mitochondria. The relative fluorescence intensity was calculated from more than 40 cells from each group. (**C**) TEM images showing representative mitochondrial morphologies of LPS and Se@SiO_2+LPS. Scale bar represents 1 μm. Red boxes indicated the mitochondria and yellow arrowheads indicated Se@SiO_2 NPs near the mitochondria, respectively. (**D**) Analysis of mitochondrial FF in each group. (**E**) Confocal fluorescence images of FITC-labeled Se@SiO_2 NPs in Beas-2B cells, shown in green; Mitochondria were labeled with MitoTracker Red CMXRos staining solution and shown in red. Yellow arrowheads indicated the distribution of Se@SiO_2 NPs around mitochondria. Scale bar represents 25 μm. NP concentration = 1 μg/mL. (**F**) The influence of our Se@SiO_2 NPs on reduced expression of mitochondrial fusion protein OPA1 and MFN2 upon LPS challenge. NP concentration = 10 μg/mL, LPS = 10 ng/mL. *p < 0.05, **p < 0.01.

AECs (Figure 4C). Furthermore, TEM images of mitochondria were processed by ImageJ software to calculate morphological parameters: the mitochondrial form factor (FF). As shown in Figure 4D, the mitochondrial FF in NPs-treated group increased significantly when compared to LPS group, indicating less fragments and more branches.

Then, we visualized the NPs under TEM and confocal microscope using synthesized fluorescein isothiocyanate (FITC)-conjugated nanoparticles to examine the cellular uptake and location of our Se@SiO_2 NPs. In TEM images of Beas-2B cells, we observed the uptake of Se@SiO_2 NPs into cytoplasm and their accumulation near mitochondria (Figure 4C). By use of confocal imaging, we detected similar phenomenon that green fluorescence-labeled NPs distributed beside the red MitoTracker-labeled mitochondria (Figure 4E).

To further investigate the mechanism underlying the changes in mitochondrial activity and morphology, we studied expressions of the mitochondrial fusion protein which regulated mitochondrial function. In the Beas-2B cells, LPS stimulation for 24 h dramatically reduced the expression of mitochondrial fusion protein, represented by optic atrophy 1 (OPA1) and Mitofusin 2 (MFN2) (Figure 4F). However, pretreated with Se@SiO_2 NPs reversed this downward trend (Figure 4F). The findings suggested that our Se@SiO_2 NPs were able to ameliorate mitochondrial

dynamics, thus mitigating mitochondrial dysfunction in LPS-challenged AECs.

Porous Se@SiO_2 NPs Showed Potent Therapeutic Activity in an ALI Model in vivo

Since Se@SiO_2 NPs exhibited strong abilities in ameliorating mitochondrial dysfunction and eliminating excessive oxidative stress in AECs, we anticipated that Se@SiO_2 might be effective on decreasing LPS-triggered lung injury in vivo. Herein, we adopted a classical mice model of ALI caused by nonlethal dose (10 mg/Kg) of LPS intranasally to induce acute injury within lung tissue. Se@SiO_2 NPs were given 1 h before LPS stimulation, and the detection was conducted 24 h after LPS challenge (Figure 5A).

Firstly, we quantified inflammatory cell infiltration and certain cytokine secretion within bronchoalveolar lavage fluid (BALF) to evaluate airway inflammatory response. Before LPS challenge, the NPs-treated mice showed similar total cells and neutrophils, but higher macrophages numbers in the BALF compared to control group (Figure 5B–D). After LPS instillation, it was found that Se@SiO_2 NPs significantly reduced the total amounts of inflammatory cells as well as neutrophils, but not macrophages within BALF of ALI mice (Figure 5B–D). These results suggested that Se@SiO_2 NPs treatment promoted macrophage infiltration while suppressed neutrophil recruitment. Pretreated with NPs also reduced the

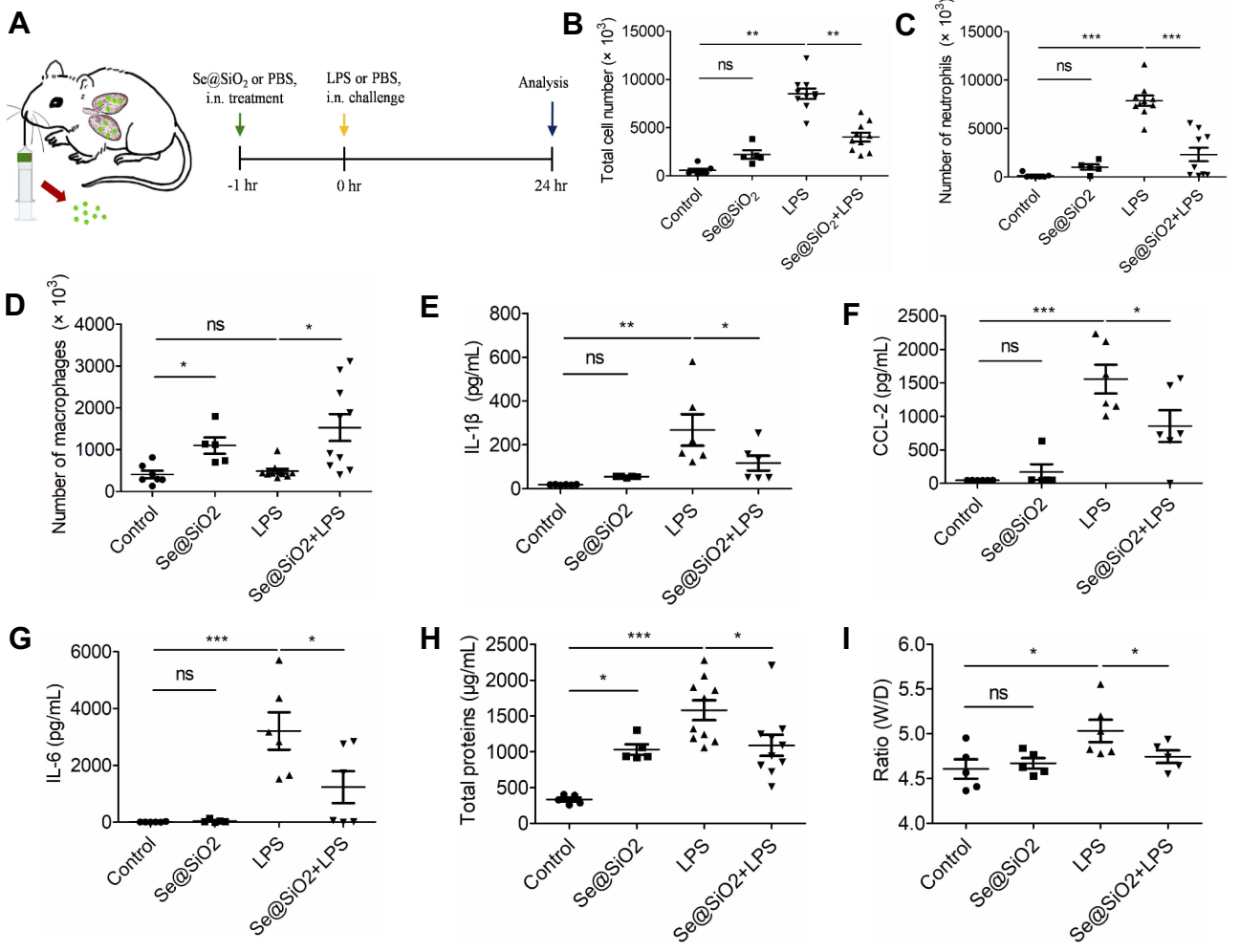

Figure 5 The inhibitory activity of Se@SiO_2 NPs in an ALI mouse model induced by LPS. (**A**) The ALI mouse model with Se@SiO_2 pretreatments (100 μg/Kg) intranasally (i.n.) 1 h before LPS (10 mg/Kg) challenge; mice were sacrificed 24 h after LPS instillation for further analysis. (**B-G**) BALF in each group were collected for the detection of total cell amounts (**B**), neutrophil numbers (**C**), macrophage counts (**D**) as well as cytokines IL-1β (**E**), CCL2 (**F**), and IL-6 (**G**) production. (**H–I**) The damage of the alveolocapillary membrane was analyzed by total protein amounts (**H**) and the lung W/D ratio (**I**) in BALF. NP concentration = 100 μg/Kg, LPS = 10 mg/Kg, *$p < 0.05$, **$p < 0.01$, ***$p < 0.001$.

Abbreviation: ns, not significant.

levels of proinflammatory cytokines IL-1β, CCL-2, and IL-6 in BALF of the ALI mice (Figure 5E–G).

As a key element in the pathogenesis of ALI, we then accessed the permeability of alveolocapillary membrane by measuring total protein in BALF and the wet-to-dry (W/D) weight ratio of the right lung. As shown in Figure 5H and I, Se@SiO_2 NPs were able to decrease total protein and W/D ratio within lungs of ALI mice. These results demonstrated that our novel NPs were potent in ameliorating the injury of alveolocapillary membrane in early stage of ALI.

In addition to BAL analysis, we also assessed the lung tissue histopathology after LPS challenge with or without Se@SiO_2 NPs pretreatment. Represented by neutrophils in alveolar space and interstitial space, proteinaceous debris within the airspaces, hyaline membrane formation as well as alveolar septal thickening (Figure 6A), we demonstrated that the total injury score in NPs-pretreated group was apparently decreased in ALI mice (Figure 6B). As for the underlying mechanisms, we discovered reduced phosphorylation of ERK1/2 and p38 as well as increased expression of OPA1, MFN2, NRF2, and NQO1 in ALI lung tissues regulated by Se@SiO_2 NPs (Figure 6C). These were highly consistent with in vitro experiments. Altogether, we suggested that porous Se@SiO_2 NPs could improve mitochondrial dynamics, control inflammatory responses as well as decrease diffuse alveolar damage within ALI lungs.

GO Annotation and KEGG Pathway Analysis of the Porous Se@SiO_2 Nanoparticles Treatment in LPS-Stimulated AECs

To further explore the biological processes regulated by Se@SiO_2 NPs in LPS-treated AECs, we conducted GO enrichment and KEGG pathway analysis. Considering the rich factor and p-value, biological process (BP), cellular component (CC), and molecular function (MF) aspects of the top 10 significant enrichment GO terms are shown in Figure 7A. We identified that the LPS responsive transcripts modulated by Se@SiO_2 NPs were largely associated with cellular response to DNA damage stimulus (GO: 0006974), regulation of cellular metabolic process (GO: 0031323) and organelle organization (GO: 0006996) (Figure 7A). From the KEGG pathway analysis, we found that NPs-regulated mRNAs mainly participated in infectious diseases (hsa05131, hsa05132, hsa05130), cancers (hsa05205, hsa05225), nervous system (hsa04721), aging (hsa04213), and immune system (hsa04670) (Figure 7B). These data supported the broad modulatory activity of the porous Se@SiO_2 NPs and their potential for clinical translation in metabolic disorders and inflammatory diseases (e.g., acute lung injury).

Discussion

Mitochondria have been widely exploited as therapeutic targets for various cancers due to their significant functional and structural differences between normal and cancer cells.[36,37] Over the years, numerous mitochondrial-targeting nanodevices have been designed as antitumor strategies and exhibited remarkable potencies.[38–40] Notably, Zhang et al[18] reported a novel mitochondria and cancer cell dual targeting polyprodrug nanoreactors, which could inhibit cellular respiration, amplify mitochondrial ROS (mtROS) and endow long-term excessive oxidative stress, eventually leading to cancer cell apoptosis. The strategy overcame several major defects that compromised efficiency, such as short lifetime, insufficient intracellular level, and limited action range of endogenous ROS, thus was considered to be promising for theranostics.[18] On the other hand, researches on nanodevices application to maintain mitochondrial homeostasis were relatively limited. Recently, Kwon and colleagues synthesized mitochondria-targeting TPP-conjugated ceria nanoparticles, which mitigated mitochondria damage, eliminated mitochondrial ROS and suppressed neuronal death, suggesting a promising strategy for the prevention and cure of Alzheimer's disease.[19] We recently fabricated a novel porous SiO_2-coated ultrasmall Se particle (Se@SiO_2 NPs), which served as a drug delivery and theranostic nanoplatform. This new developed nanodevice has proved to effectively restrain excessive oxidative stress in several disease models.[22–24,26] Accordingly, we speculated that the antioxidant effect of our Se@SiO_2 NPs was achieved by modulating mitochondria dysfunction. In the current study, we found the porous Se@SiO_2 NPs, accumulated beside mitochondria, could maintain their ROS-scavenging activity, as well as ameliorate mitochondrial dynamics, thus protecting AECs from LPS-induced acute injury (Figure 8). In addition, we used RNA-seq method and demonstrated that porous Se@SiO_2 NPs globally shifted LPS-induced gene expression profile of human AECs closer towards the normal control, among which many were related to the morphological integrity and functional stability of mitochondria. Moreover, Se@SiO_2 NPs could reduce acute inflammatory responses and attenuate lung tissue injuries in a mouse model of ALI. GO annotation and KEGG pathway analysis indicated a wide application potential for different kinds of disorders, such as

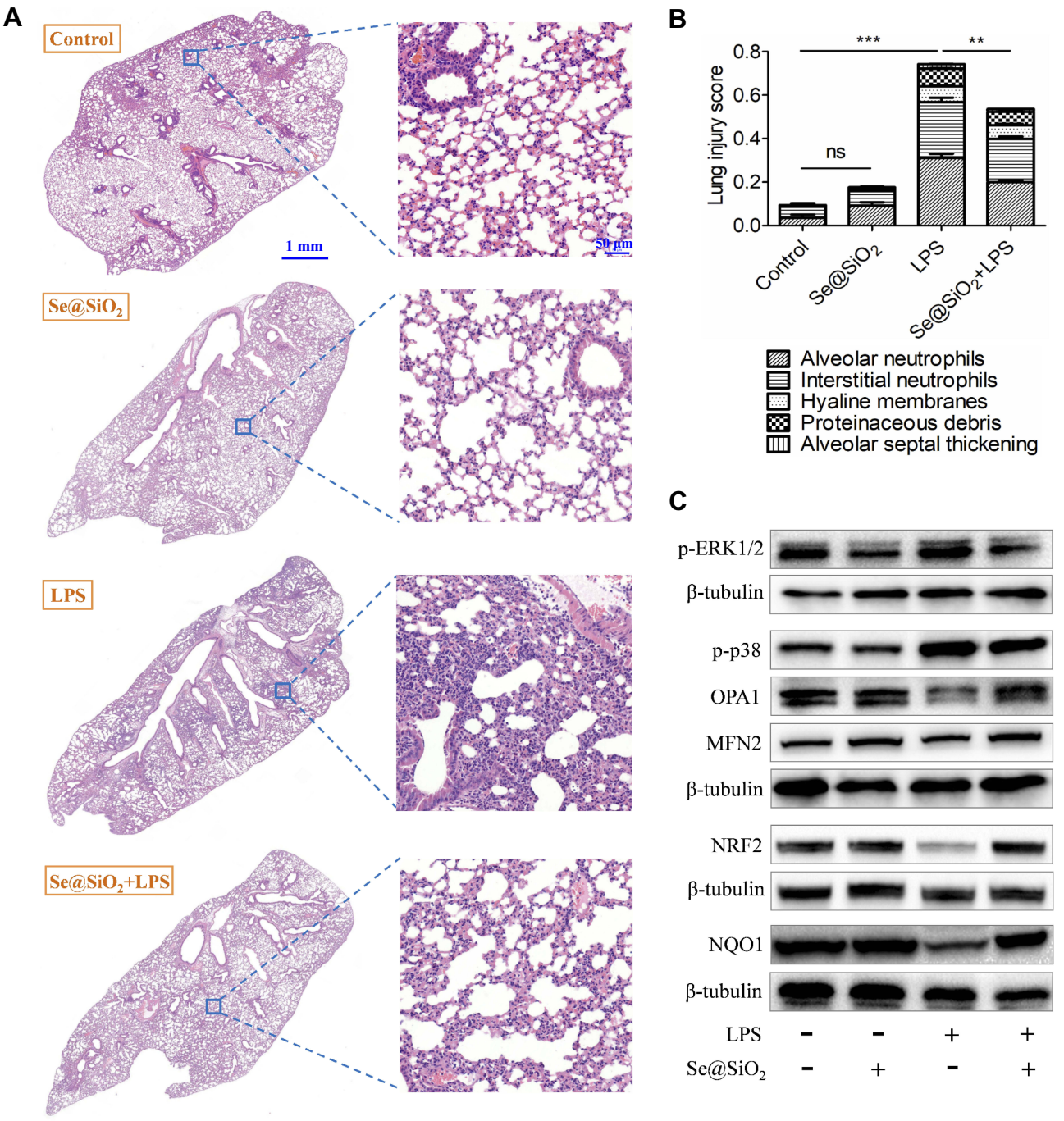

Figure 6 Protective effects of porous $Se@SiO_2$ NPs on diffuse lung injuries of ALI mice. (**A**) The typical histological photos of the lung sections stained with H&E in each group. The scale bar in the left panel represents 1 mm while that in the right panel represents 50 μm. (**B**) Lung damage in each group was evaluated by five pathophysiological features to get the total score. (**C**) The impact of $Se@SiO_2$ NPs on the expression of several proteins in lung tissues of ALI mice. NP concentration = 100 μg/Kg, LPS = 10 mg/Kg, ns = not significant, $^{**}p < 0.01$, $^{***}p < 0.001$.

infectious diseases, cancers, and nervous system disorders. These data altogether suggested a potential role of our $Se@SiO_2$ NPs for clinical applications in treating ALI/ARDS and other mitochondria-related disorders.

The application of nanodevices in modulating mitochondrial dysfunction largely depended on their mitochondrial-targeting efficiency. Nowadays, drug systems that could successfully target mitochondria were mainly achieved by coupling with mitochondria-targeted peptides[41,42] or TPPs.[12,40] However, the chemical reactions mentioned above were relatively complicated, and the organic solvent during the synthesis process was difficult to completely remove, which might cause damage to the liver, kidney, and nervous system, therefore limiting their clinical

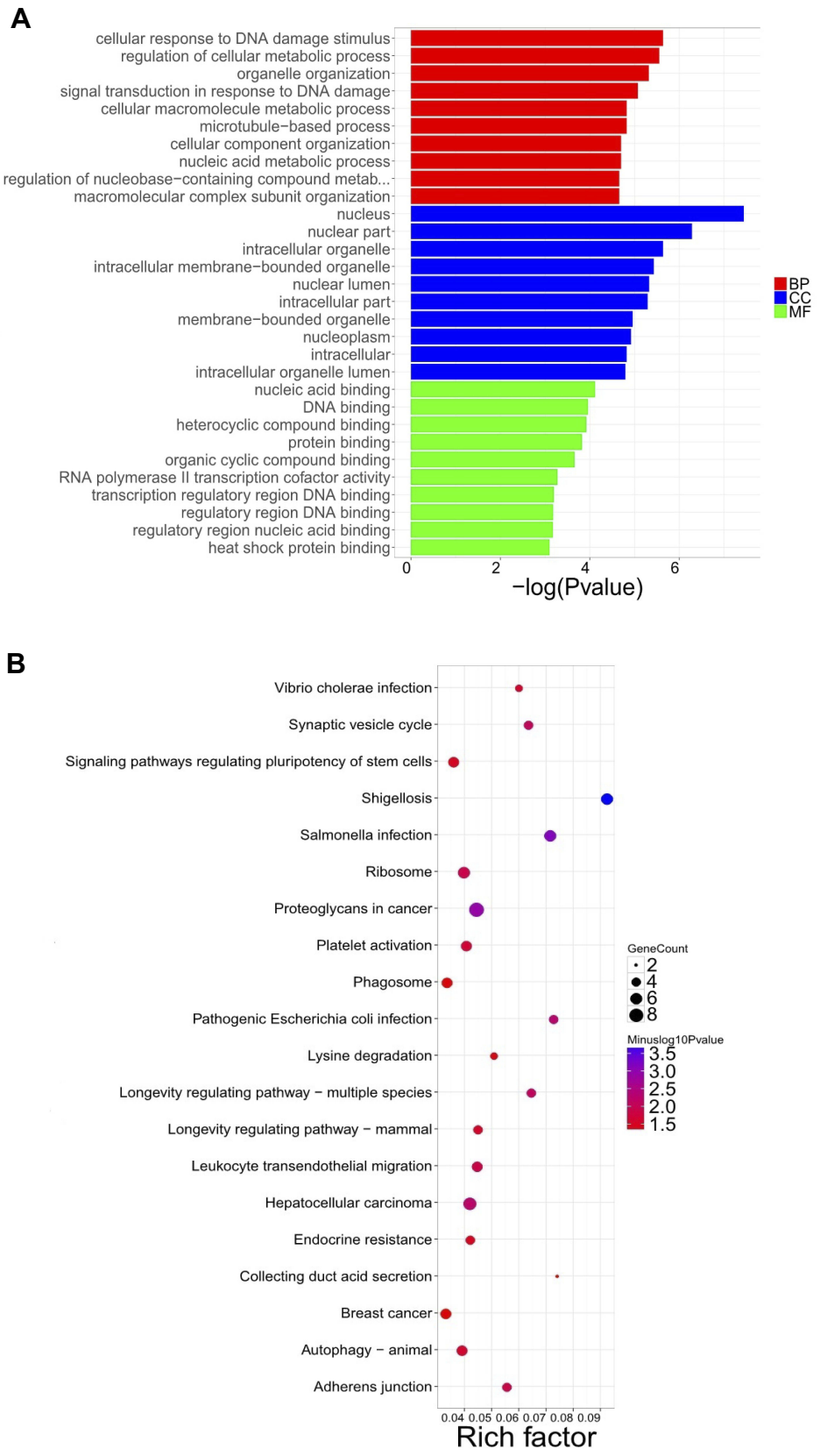

Figure 7 GO annotation and KEGG pathway analysis of the porous Se@SiO_2 NPs treatment in LPS-stimulated AECs. (**A**) GO enrichment analysis. (**B**) KEGG pathway analysis.

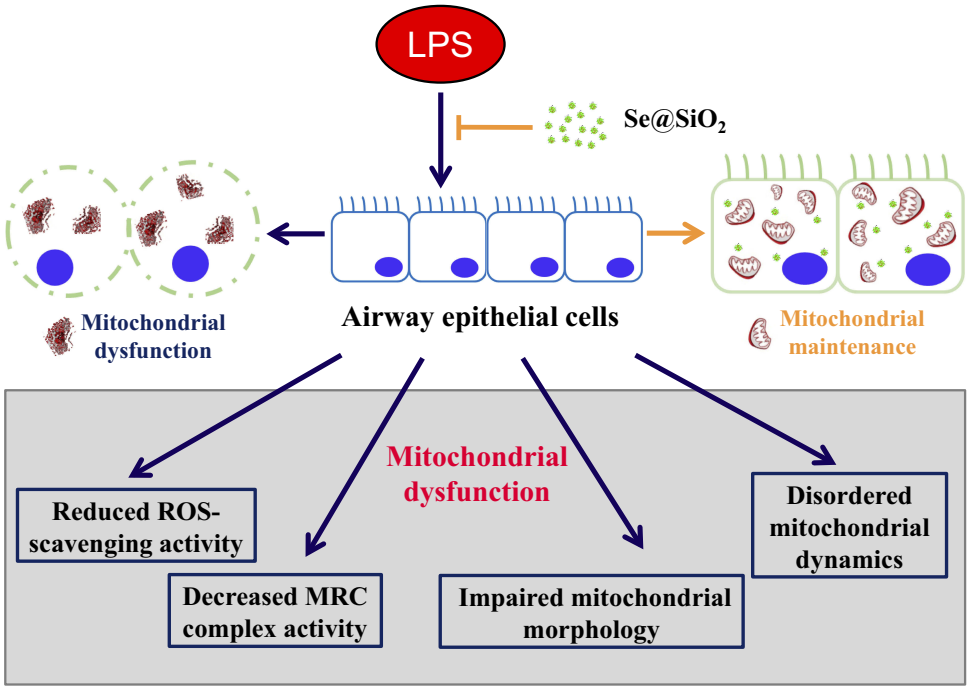

Figure 8 Diagram of the modulatory activity of porous Se@SiO_2 NPs on mitochondrial dysfunction in airway epithelial cells.

transformation prospects. Among different drug delivery systems, silicon nanoparticles attracted interests of researchers and were widely used as theranostic platforms due to their large specific surface area, uniform particle size distribution, as well as favorable biocompatibility and stability.[43] Recently, we constructed a novel Se@SiO_2 nanodevice and validated its mitochondrial-protecting effects in the present study. Meanwhile, we found that these NPs were able to enter the cytoplasm and accumulated near the mitochondria. However, we scarcely observed them inside the mitochondria, indicating the necessity to further optimize their mitochondrial-targeting efficiency. Through attaching cations and forming positively charged surface, nanoparticles could interact with the phospholipid bilayers and change mitochondrial membrane potential, thereby modifying their permeability and entering into mitochondria.[44] Accordingly, we would modulate the charge of Se@SiO_2 NPs by surface modification in order to enhance the aggregation into mitochondria in our future work. Besides, organic functional groups could be incorporated into our silica frameworks to develop organic-inorganic hybrid NPs, since the degradation rate and location of organosilica nanoparticles have been reported to be well controlled by varying the organic groups present.[45,46] These may provide solutions to the potential risk of uncontrolled degradation of the silica framework and unwanted in vivo retention.[47]

It has been demonstrated that Se@SiO_2 NPs increased the resistance of airway epithelium to LPS-induced oxidative injury and improved outcomes of ALI mice. In fact, several nanodevices have been reported to protect against this disorder through different ways.[48,49,50,51] Zhang et al prepared an anti-ICAM-1 antibodies-coated stimuli-responsive NP encapsulated with 2-[(Aminocarbonyl) amino]-5-(4-fluorophenyl)-3-thiophenecarboxamide (TPCA-1)] with the ability to target inflammatory endothelia and inhibit neutrophil transmigration, thus restraining the progression of ALI.[48] Recently, another anti-inflammatory nanomaterial, the peptide-gold nanoparticle hybrid (P12), has been exploited to specifically target innate immune cells, regulate Toll-like receptor (TLR) signaling and attenuate lung inflammatory responses.[49,51] Current nano-based therapies for ALI mainly aimed to inhibit the activation of inflammatory pathways, such as NF-κB and TLR signal transduction. However, over-attenuation or long-term suppression of these signaling might influence immune function in vivo, for instance, induce defects in antibacterial ability.[52,53] Mitochondria were suggested to facilitate cellular homeostasis by producing several redox enzymes, such as MRC complex I–III; otherwise, mitochondrial impairment might further cause damage to the entire cell.[54] Herein, we demonstrated that Se@SiO_2 NPs significantly enhanced cellular resistance

by promoting mitochondrial morphology and function stable when stimulated with LPS, thereby minimizing the side effects of single-act on immune-inflammatory pathways. In in vivo experiments, we showed that the porous Se@SiO_2 NPs reduced numbers of total inflammatory cells and neutrophils, with elevated macrophage counts in the BALF of ALI mice. This was consistent with previous understandings that elevated recruitment of alveolar macrophage modulated neutrophil infiltration and protected against LPS-induced ALI[55,56] and implied another possible explanation for the therapeutic activity of our NPs. In the near future, we would like to explore the impacts of our Se@SiO_2 NPs on other cell types within lung tissue to further elucidate mechanisms underlying the protective activity against acute injury and optimize our therapeutic regimen.

As mentioned above, mitochondrial dysfunction involved in various pathological conditions, providing a broad prospect for the clinical application of our nanodevice. For instance, chronic obstructive pulmonary disease (COPD) is defined as a common lung disorder characterized by irreversible and progressive airflow limitation; this disease is induced by chronic exposure to several noxious particles or gases, such as cigarette smoke (CS).[57] Oxidant–antioxidant imbalance is one of the leading factors involved in the pathogenesis of COPD[58] and mitochondria function of airway epithelium was dramatically disturbed in the presence of cigarette smoke extract (CSE).[59] Our preliminary data showed that the porous Se@SiO_2 NPs also decreased CSE-induced excessive mtROS production in AECs (data were not shown). Therefore, we had good reasons to believe that Se@SiO_2 NPs would become a promising candidate for the prevention and treatment of COPD. In addition, GO annotation analysis and KEGG pathway analysis also provided us evidence for the global clinical application prospects of our nanodevice. Results showed that NPs-modulated mRNAs mainly participated in infectious diseases, cancers, nervous system, and aging, which were closely related to mitochondrial dysfunction. These evidences reinforced our conclusion and gave us the confidence to continue our research in a category of disease models.

Conclusions

The present study demonstrated that the porous Se@SiO_2 NPs enhanced the resistance of airway epithelial cells against LPS-induced acute injury. Globally, Se@SiO_2 NPs shifted the LPS-induced gene expression profile of human AECs closer to the normal control. Possible mechanisms lied in protecting functional stability and preserving the structural integrity of mitochondria in AECs (Figure 8). Furthermore, this nanodevice was able to control airway inflammatory responses and attenuate tissue injuries in an LPS-induced ALI mouse model. GO annotation and KEGG pathway analysis showed broad therapeutic potentials for various disorders. This study brings new insights into mitochondria-modulating bioactive NPs, with application potential in curing ALI/ARDS or other human mitochondria-related diseases.

Abbreviations

ALI, acute lung injury; ARDS, acute respiratory distress syndrome; AEC, airway epithelial cell; NP, nanoparticle; LPS, lipopolysaccharide; ROS, reactive oxygen species; TPP, triphenylphosphonium; TEM, transmission electron microscopy; XRD, X-ray diffractometer; MRC, mitochondrial respiratory chain; CCK-8, Cell Counting Kit-8; BALF, bronchoalveolar lavage fluid; GO, Gene ontology; KEGG, Kyoto Encyclopedia of Genes and Genomes; ATP, adenosine triphosphate; SDS-PAGE, sodium dodecyl sulfate-polyacrylamide gels; TBS, tris-buffered saline; MTR, Mitotracker Red CMXRos; FPKM, fragments per kilobase of transcript per million fragments mapped; IL-1β, interlukin-1β; CCL-2, macrophage chemotactic protein-1; IL-6, interlukin-6; H&E, hematoxylin-eosin; W/D ratio, wet to dry ratio; ± SEM, mean ± standard error; ERK, extracellular-signal regulated kinase; MAPK, mitogen-activated protein kinase; NRF2, nuclear factor erythroid 2-related factor 2; NQO1, NAD(P)H quinone dehydrogenase-1; ZO-1, zonula occludens-1; E-Ca, E-cadherin; PCA, principal component analysis; FF, form factor; FITC, fluorescein isothiocyanate; mtROS, mitochondrial ROS; TLR, Toll-like receptor; COPD, chronic obstructive pulmonary disease; CSE, cigarette smoke extract.

Funding

This work was supported by National Natural Science Foundation of China (grant number: 81870064), "Gaoyuan" project of Pudong Health and Family Planning Commission (grant number: PWYgy2018-06) and Shanghai Jiao Tong University Medical and Engineering Cross Fund (grant number: YG2019QNA65).

Disclosure

The authors declare no conflict of interest in this work.

References

1. Zhang H, Feng YW, Yao YM. Potential therapy strategy: targeting mitochondrial dysfunction in sepsis. *Mil Med Res*. 2018;5(1):41.
2. Zhu Y, Dean AE, Horikoshi N, Heer C, Spitz DR, Gius D. Emerging evidence for targeting mitochondrial metabolic dysfunction in cancer therapy. *J Clin Invest*. 2018;128(9):3682–3691. doi:10.1172/JCI120844
3. Bhatti JS, Bhatti GK, Reddy PH. Mitochondrial dysfunction and oxidative stress in metabolic disorders - A step towards mitochondria based therapeutic strategies. *Biochim Biophys Acta Mol Basis Dis*. 2017;1863(5):1066–1077. doi:10.1016/j.bbadis.2016.11.010
4. Schumacker PT, Gillespie MN, Nakahira K, et al. Mitochondria in lung biology and pathology: more than just a powerhouse. *Am J Physiol Lung Cell Mol Physiol*. 2014;306(11):L962–L974. doi:10.1152/ajplung.00073.2014
5. Kellner M, Noonepalle S, Lu Q, Srivastava A, Zemskov E, Black SM. ROS signaling in the pathogenesis of acute lung injury (ALI) and acute respiratory distress syndrome (ARDS). *Adv Exp Med Biol*. 2017;967:105–137.
6. Thompson BT, Chambers RC, Liu KD. Acute respiratory distress syndrome. *N Engl J Med*. 2017;377(19):1904–1905. doi:10.1056/NEJMra1608077
7. Fan E, Brodie D, Slutsky AS. Acute respiratory distress syndrome: advances in diagnosis and treatment. *JAMA*. 2018;319(7):698–710. doi:10.1001/jama.2017.21907
8. Wu Y, Yao YM, Lu ZQ. Mitochondrial quality control mechanisms as potential therapeutic targets in sepsis-induced multiple organ failure. *J Mol Med (Berl)*. 2019;97(4):451–462. doi:10.1007/s00109-019-01756-2
9. Cui H, Xie N, Banerjee S, Ge J, Guo S, Liu G. Impairment of fatty acid oxidation in alveolar epithelial cells mediates acute lung injury. *Am J Respir Cell Mol Biol*. 2019;60(2):167–178. doi:10.1165/rcmb.2018-0152OC
10. Tojo K, Tamada N, Nagamine Y, Yazawa T, Ota S, Goto T. Enhancement of glycolysis by inhibition of oxygen-sensing prolyl hydroxylases protects alveolar epithelial cells from acute lung injury. *FASEB J*. 2018;fj201700888R.
11. Islam MN, Das SR, Emin MT, et al. Mitochondrial transfer from bone-marrow-derived stromal cells to pulmonary alveoli protects against acute lung injury. *Nat Med*. 2012;18(5):759–765. doi:10.1038/nm.2736
12. Adlam VJ, Harrison JC, Porteous CM, et al. Targeting an antioxidant to mitochondria decreases cardiac ischemia-reperfusion injury. *FASEB J*. 2005;19(9):1088–1095.
13. Feillet-Coudray C, Fouret G, Ebabe Elle R, et al. The mitochondrial-targeted antioxidant MitoQ ameliorates metabolic syndrome features in obesogenic diet-fed rats better than Apocynin or Allopurinol. *Free Radic Res*. 2014;48(10):1232–1246. doi:10.3109/10715762.2014.945079
14. Galley HF. Bench-to-bedside review: targeting antioxidants to mitochondria in sepsis. *Critical Care*. 2010;14(4):230. doi:10.1186/cc9098
15. Wang Y, Wei G, Zhang X, et al. Multistage targeting strategy using magnetic composite nanoparticles for synergism of photothermal therapy and chemotherapy. *Small*. 2018;14(12):e1702994. doi:10.1002/smll.v14.12
16. Jiang L, Li L, He X, et al. Overcoming drug-resistant lung cancer by paclitaxel loaded dual-functional liposomes with mitochondria targeting and pH-response. *Biomaterials*. 2015;52:126–139. doi:10.1016/j.biomaterials.2015.02.004
17. Tian BP, Li F, Li R, et al. Nanoformulated ABT-199 to effectively target Bcl-2 at mitochondrial membrane alleviates airway inflammation by inducing apoptosis. *Biomaterials*. 2019;192:429–439. doi:10.1016/j.biomaterials.2018.06.020
18. Zhang W, Hu X, Shen Q, Xing D. Mitochondria-specific drug release and reactive oxygen species burst induced by polyprodrug nanoreactors can enhance chemotherapy. *Nat Commun*. 2019;10(1):1704. doi:10.1038/s41467-019-09566-3
19. Kwon HJ, Cha MY, Kim D, et al. Mitochondria-Targeting ceria nanoparticles as antioxidants for Alzheimer's disease. *ACS Nano*. 2016;10(2):2860–2870. doi:10.1021/acsnano.5b08045
20. Rayman MP. The importance of selenium to human health. *Lancet*. 2000;356(9225):233–241. doi:10.1016/S0140-6736(00)02490-9
21. Spallholz JE. On the nature of selenium toxicity and carcinostatic activity. *Free Radic Biol Med*. 1994;17(1):45–64. doi:10.1016/0891-5849(94)90007-8
22. Zhu Y, Deng G, Ji A, et al. Porous Se@SiO_2 nanospheres treated paraquat-induced acute lung injury by resisting oxidative stress. *Int J Nanomedicine*. 2017;12:7143–7152. doi:10.2147/IJN.S143192
23. Liu X, Deng G, Wang Y, et al. A novel and facile synthesis of porous SiO_2-coated ultrasmall Se particles as a drug delivery nanoplatform for efficient synergistic treatment of cancer cells. *Nanoscale*. 2016;8(16):8536–8541. doi:10.1039/C6NR02298G
24. Yang BY, Deng GY, Zhao RZ, et al. Porous Se@SiO_2 nanosphere-coated catheter accelerates prostatic urethra wound healing by modulating macrophage polarization through reactive oxygen species-NF-kappaB pathway inhibition. *Acta biomaterialia*. 2019;88:392–405. doi:10.1016/j.actbio.2019.02.006
25. Matute-Bello G, Downey G, Moore BB, et al. An official American Thoracic Society workshop report: features and measurements of experimental acute lung injury in animals. *Am J Respir Cell Mol Biol*. 2011;44(5):725–738. doi:10.1165/rcmb.2009-0210ST
26. Deng G, Dai C, Chen J, et al. Porous Se@SiO_2 nanocomposites protect the femoral head from methylprednisolone-induced osteonecrosis. *Int J Nanomedicine*. 2018;13:1809–1818. doi:10.2147/IJN.S159776
27. Singh B, Li X, Owens KM, Vanniarajan A, Liang P, Singh KK. Human REV3 DNA polymerase zeta localizes to mitochondria and protects the mitochondrial genome. *PLoS One*. 2015;10(10):e0140409. doi:10.1371/journal.pone.0140409
28. Papeta N, Zheng Z, Schon EA, et al. Prkdc participates in mitochondrial genome maintenance and prevents Adriamycin-induced nephropathy in mice. *J Clin Invest*. 2010;120(11):4055–4064. doi:10.1172/JCI43721
29. Ullrich M, Assmus B, Augustin AM, et al. SPRED2 deficiency elicits cardiac arrhythmias and premature death via impaired autophagy. *J Mol Cell Cardiol*. 2019;129:13–26.
30. Onodera Y, Nam J-M, Horikawa M, Shirato H, Sabe H. Arf6-driven cell invasion is intrinsically linked to TRAK1-mediated mitochondrial anterograde trafficking to avoid oxidative catastrophe. *Nat Commun*. 2018;9(1):2682. doi:10.1038/s41467-018-05087-7
31. Palanisamy AP, Cheng G, Sutter AG, et al. Mitochondrial uncoupling protein 2 induces cell cycle arrest and necrotic cell death. *Metab Syndr Relat Disord*. 2014;12(2):132–142. doi:10.1089/met.2013.0096
32. Li Q, Hakimi P, Liu X, et al. Cited2, a transcriptional modulator protein, regulates metabolism in murine embryonic stem cells. *J Biol Chem*. 2014;289(1):251–263. doi:10.1074/jbc.M113.497594
33. Roy S, Banerjee J, Gnyawali SC, et al. Suppression of induced microRNA-15b prevents rapid loss of cardiac function in a dicer depleted model of cardiac dysfunction. *PLoS One*. 2013;8(6):e66789. doi:10.1371/journal.pone.0066789
34. Yano M. ABCB10 depletion reduces unfolded protein response in mitochondria. *Biochem Biophys Res Commun*. 2017;486(2):465–469. doi:10.1016/j.bbrc.2017.03.063
35. Kim NH, Hong BK, Choi SY, et al. Reactive oxygen species regulate context-dependent inhibition of NFAT5 target genes. *Exp Mol Med*. 2013;45:e32. doi:10.1038/emm.2013.61
36. Modica-Napolitano JS, Singh KK. Mitochondrial dysfunction in cancer. *Mitochondrion*. 2004;4(5–6):755–762. doi:10.1016/j.mito.2004.07.027

37. Wen S, Zhu D, Huang P. Targeting cancer cell mitochondria as a therapeutic approach. *Future Med Chem*. 2013;5(1):53–67. doi:10.4155/fmc.12.190
38. Shim MS, Xia Y. A reactive oxygen species (ROS)-responsive polymer for safe, efficient, and targeted gene delivery in cancer cells. *Angew Chem Int Ed Engl*. 2013;52(27):6926–6929. doi:10.1002/anie.201209633
39. Pathania D, Millard M, Neamati N. Opportunities in discovery and delivery of anticancer drugs targeting mitochondria and cancer cell metabolism. *Adv Drug Deliv Rev*. 2009;61(14):1250–1275. doi:10.1016/j.addr.2009.05.010
40. Hu Q, Gao M, Feng G, Liu B. Mitochondria-targeted cancer therapy using a light-up probe with aggregation-induced-emission characteristics. *Angew Chem Int Ed Engl*. 2014;53(51):14225–14229. doi:10.1002/anie.v53.51
41. Li J, Chen X, Xiao W, et al. Mitochondria-targeted antioxidant peptide SS31 attenuates high glucose-induced injury on human retinal endothelial cells. *Biochem Biophys Res Commun*. 2011;404(1):349–356. doi:10.1016/j.bbrc.2010.11.122
42. Huang J, Li X, Li M, et al. Mitochondria-targeted antioxidant peptide SS31 protects the retinas of diabetic rats. *Curr Mol Med*. 2013;13(6):935–945. doi:10.2174/15665240113139990049
43. Ying JY, Mehnert CP, Wong MS. Synthesis and applications of supramolecular-templated mesoporous materials. *Angew Chem Int Ed*. 1999;38(1–2):56–77. doi:10.1002/(ISSN)1521-3773
44. Rocha M, Apostolova N, Herance JR, Rovira-Llopis S, Hernandez-Mijares A, Victor VM. Perspectives and potential applications of mitochondria-targeted antioxidants in cardiometabolic diseases and type 2 diabetes. *Med Res Rev*. 2013;34(1):160–189. doi:10.1002/med.21285
45. Du X, Kleitz F, Li X, Huang H, Zhang X, Qiao S-Z. Disulfide-bridged organosilica frameworks: designed, synthesis, redox-triggered biodegradation, and nanobiomedical applications. *Adv Funct Mater*. 2018;28(26):1707325. doi:10.1002/adfm.201707325
46. Wu M, Meng Q, Chen Y, et al. Large pore-sized hollow mesoporous organosilica for redox-responsive gene delivery and synergistic cancer chemotherapy. *Adv Mater*. 2016;28(10):1963–1969. doi:10.1002/adma.201505524
47. Wu J, Williams GR, Niu S, Gao F, Tang R, Zhu L-M. A multifunctional biodegradable nanocomposite for cancer theranostics. *Adv Sci (Weinh)*. 2019;6(14):1802001. doi:10.1002/advs.201802001
48. Zhang CY, Lin W, Gao J, et al. pH-responsive nanoparticles targeted to lungs for improved therapy of acute lung inflammation/injury. *ACS Appl Mater Interfaces*. 2019;11(18):16380–16390. doi:10.1021/acsami.9b04051
49. Xiong Y, Gao W, Xia F, et al. Peptide-gold nanoparticle hybrids as promising anti-inflammatory nanotherapeutics for acute lung injury: in vivo efficacy, biodistribution, and clearance. *Adv Healthc Mater*. 2018;7(19):e1800510. doi:10.1002/adhm.v7.19
50. Zhao H, Zeng Z, Liu L, et al. Polydopamine nanoparticles for the treatment of acute inflammation-induced injury. *Nanoscale*. 2018;10(15):6981–6991. doi:10.1039/C8NR00838H
51. Gao W, Wang Y, Xiong Y, et al. Size-dependent anti-inflammatory activity of a peptide-gold nanoparticle hybrid in vitro and in a mouse model of acute lung injury. *Acta biomaterialia*. 2019;85:203–217. doi:10.1016/j.actbio.2018.12.046
52. Miles SA, Conrad SM, Alves RG, Jeronimo SM, Mosser DM. A role for IgG immune complexes during infection with the intracellular pathogen Leishmania. *J Exp Med*. 2005;201(5):747–754. doi:10.1084/jem.20041470
53. Muller U, Stenzel W, Kohler G, et al. IL-13 induces disease-promoting type 2 cytokines, alternatively activated macrophages and allergic inflammation during pulmonary infection of mice with Cryptococcus neoformans. *J Immunol*. 2007;179(8):5367–5377. doi:10.4049/jimmunol.179.8.5367
54. Lopez-Otin C, Blasco MA, Partridge L, Serrano M, Kroemer G. The hallmarks of aging. *Cell*. 2013;153(6):1194–1217. doi:10.1016/j.cell.2013.05.039
55. Beck-Schimmer B, Schwendener R, Pasch T, Reyes L, Booy C, Schimmer RC. Alveolar macrophages regulate neutrophil recruitment in endotoxin-induced lung injury. *Respir Res*. 2005;6:61. doi:10.1186/1465-9921-6-61
56. Xu W, Zhu Y, Ning Y, et al. Nogo-B protects mice against lipopolysaccharide-induced acute lung injury. *Sci Rep*. 2015;5:12061. doi:10.1038/srep12061
57. Singh D, Agusti A, Anzueto A, et al. Global strategy for the diagnosis, management, and prevention of chronic obstructive lung disease: the GOLD science committee report 2019. *Eur Respir J*. 2019;53(5). doi:10.1183/13993003.00164-2019
58. Fischer BM, Voynow JA, Ghio AJ. COPD: balancing oxidants and antioxidants. *Int J Chron Obstruct Pulmon Dis*. 2015;10:261–276. doi:10.2147/COPD
59. van der Toorn M, Slebos DJ, de Bruin HG, et al. Cigarette smoke-induced blockade of the mitochondrial respiratory chain switches lung epithelial cell apoptosis into necrosis. *Am J Physiol Lung Cell Mol Physiol*. 2007;292(5):L1211–L1218. doi:10.1152/ajplung.00291.2006